NASA/TM—2005-213856 AIAA–2005–3989

Evaluation of an Active Clearance Control System Concept

Bruce M. Steinetz
Glenn Research Center, Cleveland, Ohio

Scott B. Lattime
The Timken Company, Canton, Ohio

Shawn Taylor
University of Toledo, Toledo, Ohio

Jonathan A. DeCastro
QSS Group, Inc., Cleveland, Ohio

Jay Oswald
J&J Technical Solutions, Cleveland, Ohio

Kevin J. Melcher
Glenn Research Center, Cleveland, Ohio

November 2005

The NASA STI Program Office . . . in Profile

Since its founding, NASA has been dedicated to the advancement of aeronautics and space science. The NASA Scientific and Technical Information (STI) Program Office plays a key part in helping NASA maintain this important role.

The NASA STI Program Office is operated by Langley Research Center, the Lead Center for NASA's scientific and technical information. The NASA STI Program Office provides access to the NASA STI Database, the largest collection of aeronautical and space science STI in the world. The Program Office is also NASA's institutional mechanism for disseminating the results of its research and development activities. These results are published by NASA in the NASA STI Report Series, which includes the following report types:

- TECHNICAL PUBLICATION. Reports of completed research or a major significant phase of research that present the results of NASA programs and include extensive data or theoretical analysis. Includes compilations of significant scientific and technical data and information deemed to be of continuing reference value. NASA's counterpart of peer-reviewed formal professional papers but has less stringent limitations on manuscript length and extent of graphic presentations.

- TECHNICAL MEMORANDUM. Scientific and technical findings that are preliminary or of specialized interest, e.g., quick release reports, working papers, and bibliographies that contain minimal annotation. Does not contain extensive analysis.

- CONTRACTOR REPORT. Scientific and technical findings by NASA-sponsored contractors and grantees.

- CONFERENCE PUBLICATION. Collected papers from scientific and technical conferences, symposia, seminars, or other meetings sponsored or cosponsored by NASA.

- SPECIAL PUBLICATION. Scientific, technical, or historical information from NASA programs, projects, and missions, often concerned with subjects having substantial public interest.

- TECHNICAL TRANSLATION. English-language translations of foreign scientific and technical material pertinent to NASA's mission.

Specialized services that complement the STI Program Office's diverse offerings include creating custom thesauri, building customized databases, organizing and publishing research results . . . even providing videos.

For more information about the NASA STI Program Office, see the following:

- Access the NASA STI Program Home Page at ***http://www.sti.nasa.gov***

- E-mail your question via the Internet to help@sti.nasa.gov

- Fax your question to the NASA Access Help Desk at 301–621–0134

- Telephone the NASA Access Help Desk at 301–621–0390

- Write to:
  NASA Access Help Desk
  NASA Center for AeroSpace Information
  7121 Standard Drive
  Hanover, MD 21076

NASA/TM—2005-213856 AIAA–2005–3989

Evaluation of an Active Clearance Control System Concept

Bruce M. Steinetz
Glenn Research Center, Cleveland, Ohio

Scott B. Lattime
The Timken Company, Canton, Ohio

Shawn Taylor
University of Toledo, Toledo, Ohio

Jonathan A. DeCastro
QSS Group, Inc., Cleveland, Ohio

Jay Oswald
J&J Technical Solutions, Cleveland, Ohio

Kevin J. Melcher
Glenn Research Center, Cleveland, Ohio

Prepared for the
41st Joint Propulsion Conference and Exhibit
cosponsored by the AIAA, ASME, SAE, and ASEE
Tucson, Arizona, July 10–13, 2005

National Aeronautics and
Space Administration

Glenn Research Center

November 2005

Acknowledgments

The authors would like to acknowledge the support of NASA Glenn's Ultra-efficient Engine Technology (UEET) projects Intelligent Propulsion Systems and Foundation Technologies (IPSFT) and Propulsion 21 for their financial support. The authors also acknowledge the contributions of the following people: Malcolm Robbie, Art Erker, and Tobie Mintz for their design and fabrication support; Richard Tashjian, Kevin McCormick, Tom Lawrence, Mike McGhee, and Joe Wisniewski for their technical assistance during the test rig installation and troubleshooting. And finally, the authors acknowledge Keith Blackwell for his efforts in characterizing the stepper motor load versus speed characteristics, and Robert Hendricks and Chris Daniels for their thoughtful review of the manuscript.

Available from

NASA Center for Aerospace Information
7121 Standard Drive
Hanover, MD 21076

National Technical Information Service
5285 Port Royal Road
Springfield, VA 22100

Available electronically at http://gltrs.grc.nasa.gov

Evaluation of an Active Clearance Control System Concept

Bruce M. Steinetz
National Aeronautics and Space Administration
Glenn Research Center
Cleveland, Ohio 44135

Scott B. Lattime
The Timken Company
Canton, Ohio 44706

Shawn Taylor
University of Toledo
Toledo, Ohio 43606

Jonathan A. DeCastro
QSS Group, Inc.
Cleveland, Ohio 44135

Jay Oswald
J&J Technical Solutions
Cleveland, Ohio 44130

Kevin J. Melcher
National Aeronautics and Space Administration
Glenn Research Center
Cleveland, Ohio 44135

Abstract

Reducing blade tip clearances through active tip clearance control in the high pressure turbine can lead to significant reductions in emissions and specific fuel consumption as well as dramatic improvements in operating efficiency and increased service life. Current engines employ scheduled cooling of the outer case flanges to reduce high pressure turbine tip clearances during cruise conditions. These systems have relatively slow response and do not use clearance measurement, thereby forcing cold build clearances to set the minimum clearances at extreme operating conditions (e.g., takeoff, reburst) and not allowing cruise clearances to be minimized due to the possibility of throttle transients (e.g., step change in altitude). In an effort to improve upon current thermal methods, a first generation mechanically-actuated active clearance control (ACC) system has been designed and fabricated. The system utilizes independent actuators, a segmented shroud structure, and clearance measurement feedback to provide fast and precise active clearance control throughout engine operation.

Ambient temperature performance tests of this first generation ACC system assessed individual seal component leakage rates and both static and dynamic overall system leakage rates. The ability of the nine electric stepper motors to control the position of the seal carriers in both open- and closed-loop control modes for single and multiple cycles was investigated. The ability of the system to follow simulated engine clearance transients in closed-loop mode showed the system was able to track clearances to within a tight tolerance (≤ 0.001 in. error).

I. Introduction

Gas path sealing continues to be a fundamental concern in aircraft and ground-based turbine engines. Technical drivers include the need to operate the engines under increasingly more demanding temperature and pressure conditions at high efficiency and to minimize maintenance requirements to keep operating costs at their minimum. Blade tip sealing has remained a challenging problem since the development of the gas turbine engine. Environmental conditions at the tip seal location include gas temperatures up to 2500 °F, pressures up to 600 psi, high surface speeds (1900 fps), as well as unburned jet fuel and contaminants (dirt, sand, etc.) that make for very challenging surroundings for a controllable seal design. Clearances change during engine operation as a result of both mechanical (pressure and rotational) loads and thermal loads. Discrete structural mounts coupled with thermal and flight loads result in non-uniform distortions and hence non-uniform clearances.

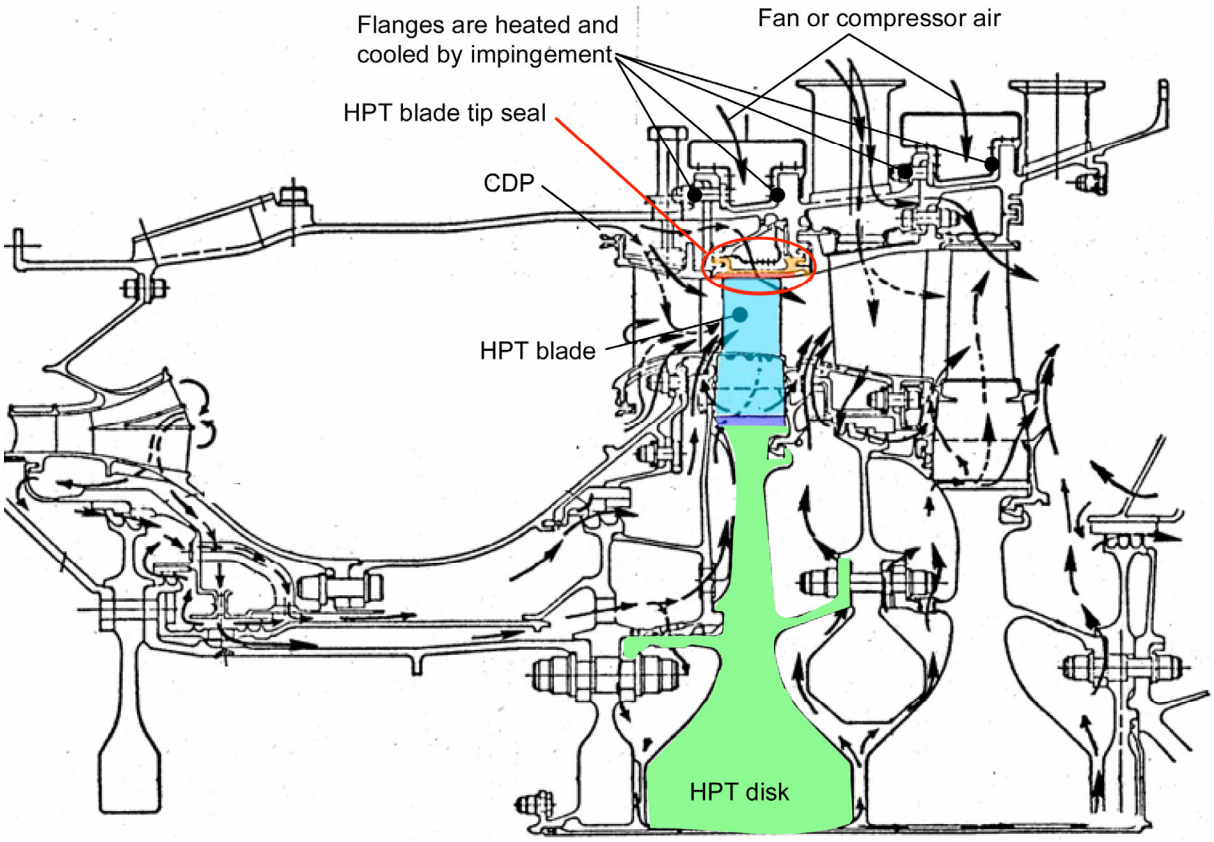

Figure 1.—HPT blade tip seal location in a modern gas turbine engine.[1]

Designers of clearance control schemes must properly account for all of these effects to implement a successful active clearance control (ACC) system.

Improved blade-tip sealing in both the high pressure compressor (HPC) and high pressure turbine (HPT) can provide dramatic reductions in specific fuel consumption (SFC), compressor stall margin and engine efficiency as well as increased payload and mission range capabilities. Implementation of active clearance control systems, especially in the HPT, can dramatically improve engine service life or time-on-wing.

A. Background

Figure 1 shows the high pressure HPT blade tip seal location in a modern gas turbine engine.[1] The figure shows a cross section of the combustor and two-stage HPT. The turbine disk, blade, and tip seal of the first-stage turbine are labeled. Blade tip or outer air seals line the inside of the stationary case forming a shroud around the rotating blades, limiting the gas that spills over the tips. Blade tip clearance varies over the operating points of the engine (e.g., ground idle, takeoff, cruise, decel, etc.) as well as over the cycle life of the engine. These clearance variations are due to a number of loads on both static and rotating parts and wear of these parts.

Load mechanisms can be separated into two categories, namely engine (power-induced) loads and flight loads. Engine loads include centrifugal, thermal, internal engine pressure, and thrust loads. Flight loads include inertial (gravitational), aero-dynamic (external pressure), and gyroscopic loads. Engine loads can produce both axisymmetric and asymmetric clearance changes (see fig. 2). Flight loads generally produce asymmetric clearance changes. Load mechanisms generally act to temporarily alter blade tip clearance, wear mechanisms permanently change tip clearance. The ACC system must be designed to handle even the worst case transient conditions such as a stop-cock event where the engine is shutdown in-flight and allowed to windmill for a while followed by restart to full power.

The backside of the HPT shroud (blade outer-air-seal) is generally cooled with compressor discharge air (T3 air: 1200 to 1300 °F). This cooling is necessary for the shroud segments to survive the 2500 °F and higher rotor inlet gas temperatures. The cooling air is also used to purge the leading and trailing edges of the shroud segments, providing a positive back-flow margin from the hot rotor inlet flow. This cooling flow is shown in figure 3 for the first stage shroud of a two-stage HPT. The pressures surrounding the shroud segment can be expressed as a function of the compressor discharge pressure (CDP; P3). Flow path pressure adjacent to the HPT shroud varies axially due to the

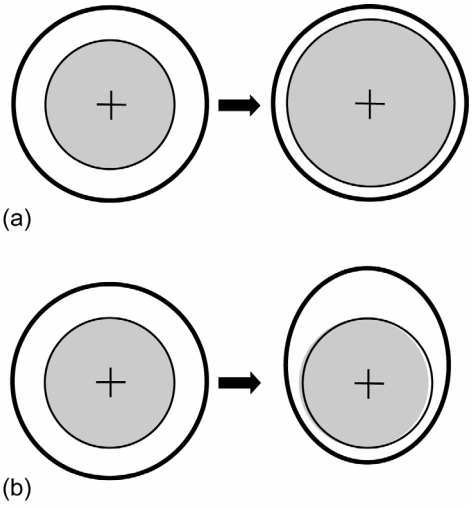

Figure 2.—(a) Axisymmetric clearance change, (b) asymmetric clearance change.

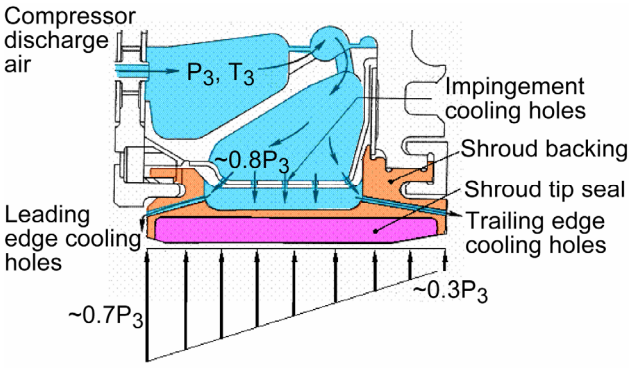

Figure 3.—Axial pressure distribution across HPT blade tip seal cross section.[2]

work extracted by the turbine blades. For large commercial engines, the pressure of the cooling air behind the shroud is about 60 to 80 percent of P3 pressure.[2] Pressure in the tip clearance region varies axially from the leading to the trailing edge of the shroud about 70 to 30 percent of the P3, respectively. To maintain a positive backflow margin from the rotor inlet air, the cooling pressure on the backside of the shroud must always be higher than the rotor inlet side. The radial pressure difference across the shroud creates a load inward toward the shaft centerline. A resultant moment also exists on the shroud that is created by the non-uniform axial pressure distribution. P3 pressure is highest during maximum thrust events such as takeoff and re-accel. For large commercial engines this translates to a maximum cooling air pressure differential of up to 150-psi across the shroud.

Wear mechanisms of blade tip seals can be generally separated into two categories, namely, rubbing (blade incursion), and erosion. Blade rubs and erosion are expected to occur throughout the service life of an engine. Engine build clearances are in fact sometimes chosen to operate line-to-line at extreme operating conditions (e.g., takeoff, re-accel). In this case, manufacturers set cold-build clearances such that during the engine green-state ("run-in") the blades will lightly rub the seal shrouds thereby achieving tight clearances at one operating point and mitigating the effects of manufacturing tolerance stack-up. Rubs can also contribute to accelerating the effects of both erosion and thermal fatigue by wearing protective coatings (e.g., thermal barrier coatings) or distorting cooling passages of the blade tips during an incursion event.

Lattime and Steinetz[2] provided a comprehensive review of the mechanisms of tip clearance variation, their effects in gas turbine engines, methods of controlling tip clearance and the benefits associated with reducing tip clearance. Kawecki[3] presented trade studies of a variety of approaches for active clearance control identifying a variety of fast-acting mechanical and novel thermal control systems. Melcher and Kypuros[4] outlined NASA Glenn's general approach for developing a fast-response ACC system and DeCastro and Melcher[5] examined the control systems requirements for fast acting ACC systems.

B. Benefits of Active Clearance Control

Blade tip clearance directly influences gas turbine performance, efficiency, and life. Reducing air leakage over the blade tips increases turbine efficiency and permits the engine to meet performance and thrust goals with less fuel burn and lower rotor inlet temperatures. Running the turbine at lower temperatures increases the cycle life of hot section components, which in turn, increases engine service life by increasing the time between overhauls.

Lattime and Steinetz,[6] GE,[7] and Wiseman and Guo[8] provide overviews of the many benefits of advanced active clearance control systems. Some of the more noteworthy benefits of implementing fast mechanical ACC systems in the HPT of a modern high bypass engine are provided herein for completeness. In terms of fuel savings, a reduction in of 0.010-in tip clearance results in ~0.8 to 1 percent decrease in specific fuel consumption. By reducing fuel burn significant reductions in NO_x, CO, and CO_2 emissions are also possible. Reducing tip clearances by 0.010-in improves exhaust gas temperature (EGT) ~10 °C. Deterioration of EGT margin is the primary reason for aircraft engine removal from service. Running the engine at lower operating temperature can result in increased life of hot section components and engine time-on-wing (up to 1000 cycles). Additional benefits include increased payload and mission range capabilities.

C. Study Objectives

This work is part of a larger research effort to develop approaches for clearance control systems for use in the HPT section of large commercial aircraft engines to improve

upon the case-cooling methods employed today. The objective of the current work is to present the preliminary evaluation of a first generation mechanical active clearance control (ACC) system that utilizes independent actuators to position a series of seal carriers or hangars that would support seal segments or shrouds in a future engine system.

Specific test objectives of this study include the evaluation of:

- Individual component seal leakages (e.g., actuator rod piston rings, face seals, flexure/spline seals) under engine simulated pressure conditions at ambient temperature.
- Overall system leakage both statically and during motion.
- Candidate actuators' ability to position the seal carriers at the required rate, accuracy, and repeatability under engine simulated pressure conditions.
- Candidate clearance sensors as part of the ACC closed-loop feedback control system.

II. Test Apparatus and Procedures

A. Apparatus

An active clearance control system test rig has been developed and installed (fig. 4). The key features of the test rig examined during this study are summarized below. For a comprehensive review of the test rig design approach, the reader is directed to Lattime and Steinetz.[6]

1. General Overview

The ACC test rig simulates the environment surrounding the backsides of the turbine shroud segments. The purpose of the test rig is to evaluate actuation systems in a "static" environment without blade rotation. The rig design concentrated on simulating the temperature and pressure conditions that exist on the backsides of the seal segments, without the need for a rotating turbine, which greatly simplified the rig design. Rig specifications were chosen to closely simulate engine requirements. Table 1 compares the main characteristics of both the ACC test rig and a typical modern high bypass ratio engine.

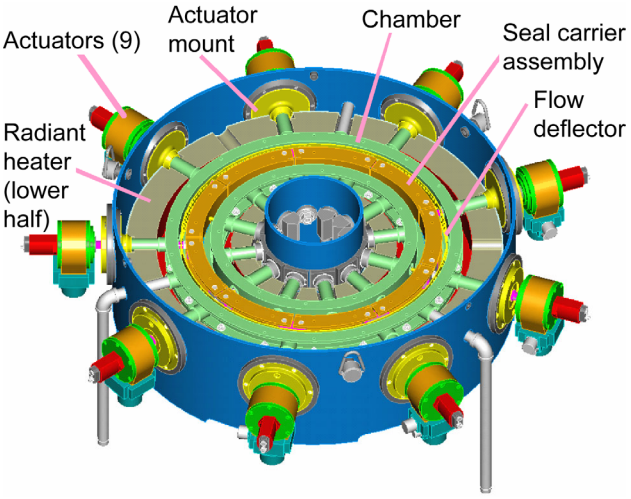

Figure 4.—ACC test rig with housing lid and chamber cover plate removed for clarity.

The general design of the test rig is shown in figures 4 to 7. The rig main housing consists of two concentric cylinders, which form an annular cavity. An annular radiant heater made of upper and lower halves surrounds the seal pressure chamber to simulate the HPT tip seal backside temperature (T3) and pressure (P3) environment. At the heart of the rig is a segmented shroud structure (seal carrier) that would structurally support the tip seal shroud segments in the engine. Radial movement of the seal carriers controls the effective position/diameter of the seal shroud segments, thereby controlling blade tip clearance. The carrier segments

TABLE 1.—COMPARISON OF ACC RIG DESIGN AND A TYPICAL MODERN HIGH BYPASS RATIO ENGINE OPERATING CHARACTERISTICS

Parameter	ACC Rig Design	Reference Engine
Shroud backside pressure (psia)	135	500
Pressure differential (psid)	120	150
Shroud Backside temperature		
Current (°F)	1000	1250
Future (°F)	1250 to 1300	1250 to 1300
Diameter (in.)	20	30
Shroud face width (in.)	2	2
Number of shrouds/seal carriers	9	16
Pressure induced load on actuator (at pressure differential) (lbf)	1650	1750
Clearance change (e.g., stroke) (in.)	0.190	0.05 nom.
Clearance change rate (in/sec)	0.01	0.01
Clearance Measurement Technique		
Current	capacitance	not used
Future (under development)	microwave	capacitance/ microwave

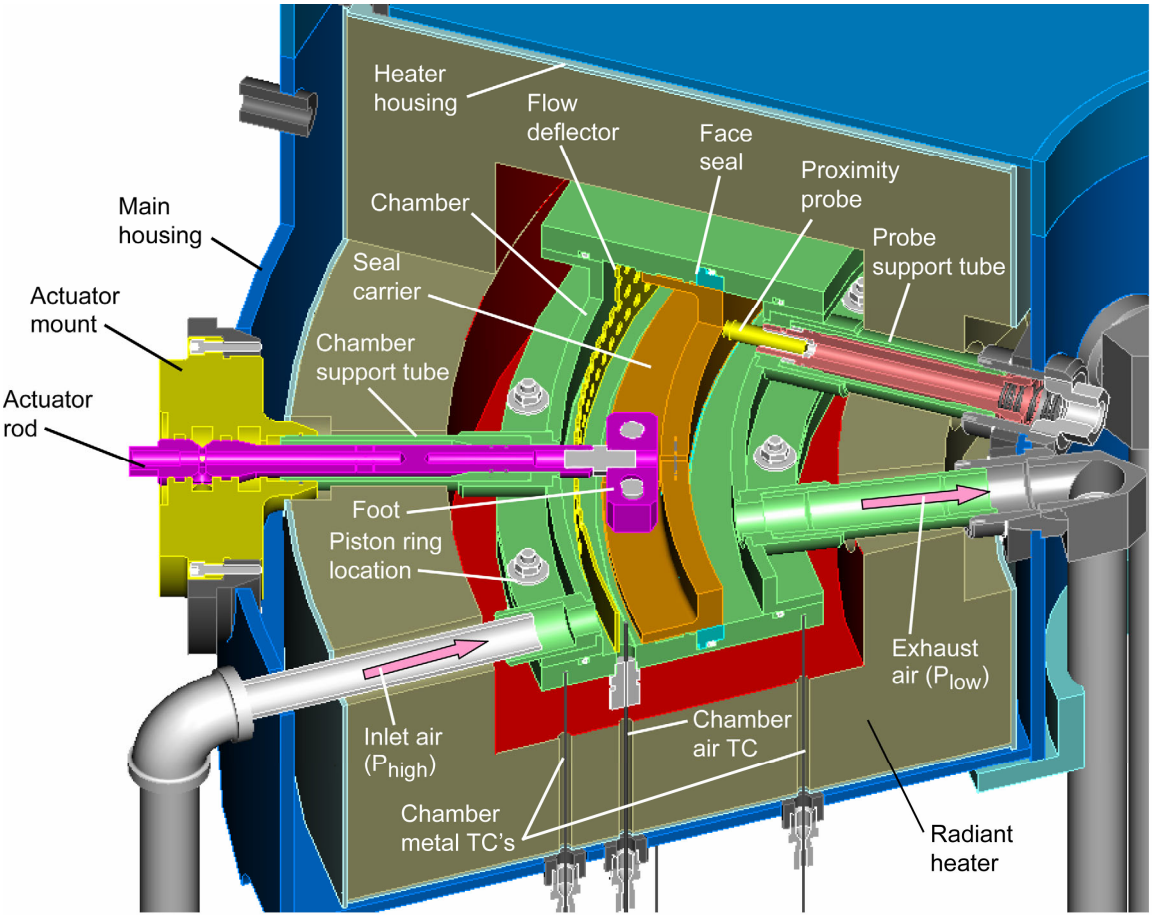

Figure 5.—ACC cut-away showing detail for one of nine actuator rods and attachment foot, actuator mount, seal carriers, proximity probe clearance sensor, inlet air supply pipe, air flow directions, and radiant heater.[6]

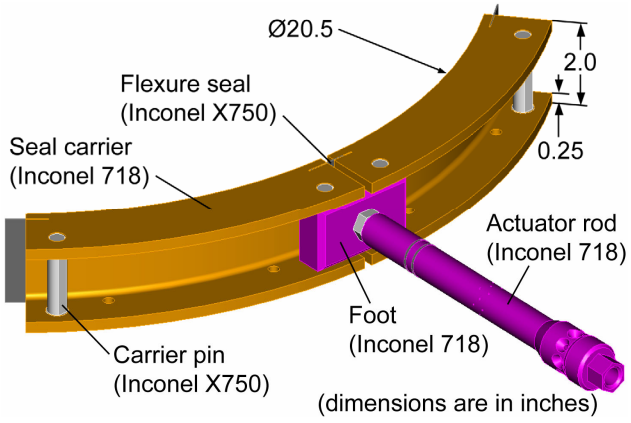

Figure 6.—Actuator rod foot, two adjacent seal carriers, flexure seals, materials, and nominal dimensions in inches.

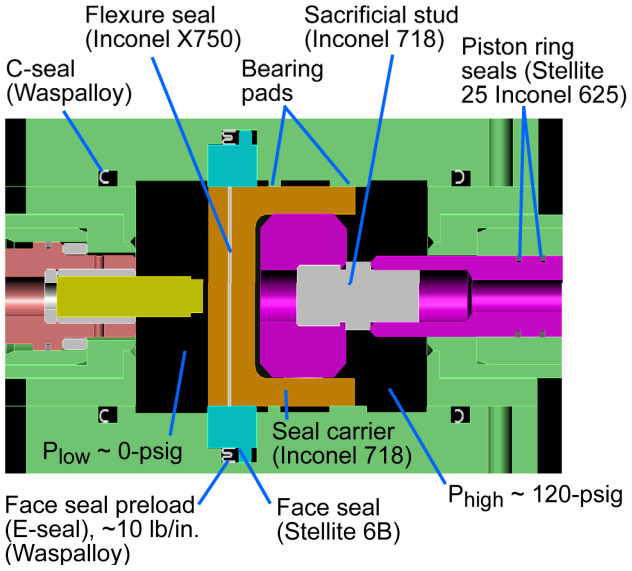

Figure 7.—Chamber detail showing seal carrier and adjacent face seals with E-seal preloader, actuator rod piston ring seals (2 places), chamber cover C-rings (4 places), the materials used in construction, and chamber high and low pressures.

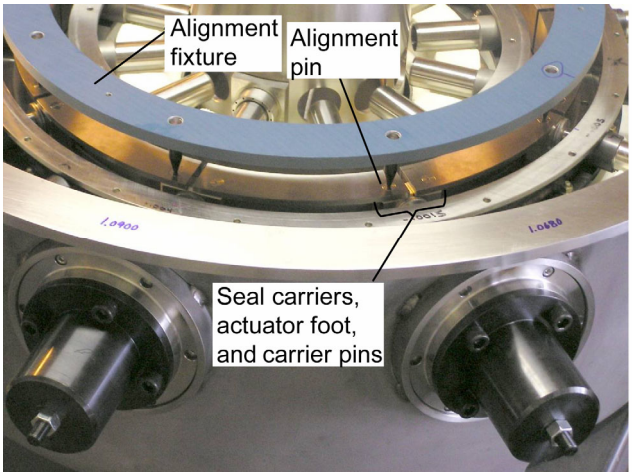

Figure 8.—ACC test rig with carrier alignment fixture installed. Note gage pins insert into precision centering holes in carrier pins. Alignment fixture used to set nominal or "home" position for all carrier segments.

are secured to one another through a pinned and slotted link as shown in figure 6. This link (or "foot") positions the carrier segments radially while allowing relative circumferential movement or dilation of the seal carrier segments. Figure 5 shows that the carrier segment is supported by two independent actuator rods. A photograph of test rig is shown in figure 8. Here the precision alignment fixture used to establish concentricity of all of the seal carriers relative to the rig centerline is installed. Tapered gage pins mounted in the alignment fixture engage precision alignment holes machined in the ends of the carrier pins. This alignment fixture or "gage plate" was used at the beginning of each test to set the nominal or "home" position for subsequent tests.

2. Chamber and Seal Detail

A pressurized chamber encloses the carrier segments inside the annular heater through which pressurized air (heated for future tests) is supplied to simulate the P3 cooling/purge air pressure on the seal carrier backsides. The pressurized air is sealed along the sides of the seal carrier segments by contacting face seals that are energized via metal "E-seals" imbedded in the upper and lower chamber plates (figs. 5 and 7). The joints between adjoining carrier segments are sealed with thin flexure seals otherwise known as spline seals (figs. 6 and 7). The face seal width was selected to seal the sliding interface between the edges of the flexure seals as they move radially inward/outward during actuation. The nine actuator rods are sealed using two sets of concentric piston ring seals. A series of radial tubes projecting outward from the chamber's inner and outer side walls serve as supports, air supply and exhaust ports, probe fixtures, and the actuator rod guides. These are sealed in their respective bosses via a shrink fit qualified during hydro-testing. The chamber functions to support and align the carrier segments and actuator rods, as well as to house instrumentation and to seal the pressurized air from the radiant heater which is not designed to carry any pressure loading. The chamber cover plates are sealed using inner- and outer-flange C-rings. Only the outer C-rings carry pressure during operation. The pipes supplying high pressure to the chamber (fig. 5) are sealed using two sets of concentric piston ring seals.

3. Actuators and Position Measurement

Electric stepper motors were used to position the seal carriers for the current set of tests. Each stepper motor is equipped with a quadrature encoder to measure both shaft rotational position and direction of motion. A complete list of specifications is found in table 2. The stepper motors are rated for 500 lbf of actuation force which limited the maximum chamber pressure that could be tested. Although calculations indicated that chamber pressures of 35 psig would result in 500 lbf actuator loads, actual tests indicated that the practical upper pressure was in the 20 to 30-psig range. It is expected that this noted difference is due to component friction. Stepper motors were selected as low-cost first generation actuators because of their high reliability and conduciveness to accurate position control. These actuators are therefore useful in evaluating the kinematics, seals, sensors, and control electronics under moderate loading conditions. Researchers are procuring a series of servo-hydraulic actuators designed to be able to handle the full 120 psig test pressure. These servo-hydraulic actuators will come equipped with linear variable differential transducers (LVDTs) to accurately measure actuator piston location.

TABLE 2.—STEPPER MOTOR SPECIFICATIONS

Maximum load capability (lbf)	500
Stroke (in.)	0.5
Displacement resolution: without micro-stepping (in.)	0.0005
Displacement resolution: with micro-stepping (in.)	10 micro steps, 0.00005
Encoder resolution (in.)	0.000125
Voltage (V)	24
Current draw-peak (amps)	1.4 max
Weight (lb)	5
Manufacturer	Haydon Switch and Instrument Inc.
Model no.	87H43–12–002

The stepper motor shafts were connected to the actuator rods through a coupling, as shown in figure 9. The coupling was manufactured with two diameters to serve two additional purposes: (1) as a mechanical stop to prevent excessive axial motion; and (2) as a convenient means to measure absolute positions of the actuator shaft relative to the actuator mount. The actuators were mounted to the mounting flanges through a series of stand-offs.

4. Instrumentation

A variety of thermocouples, pressure transducers and flow meters were used to collect the necessary data. Table 3 provides a list of the transducer specifications and their

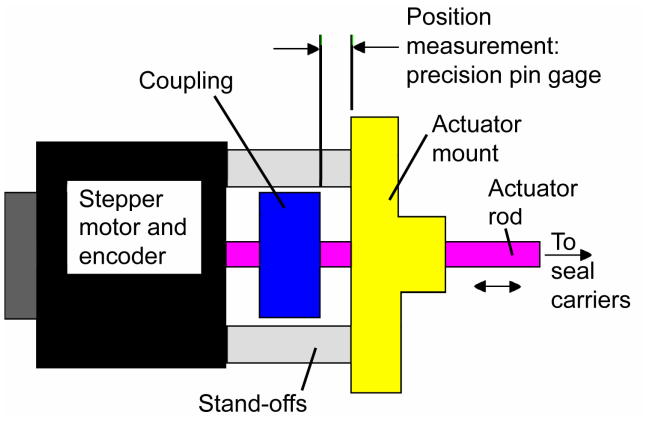

Figure 9.—Stepper motor mounting arrangement showing means for measuring actuator shaft/coupling position relative to the actuator mount.

TABLE 3.—INSTRUMENTATION SPECIFICATIONS

Thermocouples	Type K
Manufacturer	Omega
Accuracy (°F)	± 4
Range (°F)	–328 to 2282
Pressure Transducers	
Manufacturer	Druck
Model no.	PMP4010
Accuracy (psi)	0.12
Range (psi)	0 to 300
Flow meters	
Low Range	
Manufacturer	Teledyne-Hastings
Model no.	HFM-200
Accuracy (SCFM; lbm/s)	0.2; 0.00027
Range (SCFM; SLPM)	173, 6.11
High Range	
Manufacturer	Teledyne-Hastings
Model no.	HFM 200 + 3000 SLPM LFE
Accuracy (SCFM; lbm/s)	1.06; 0.0014
Range (SCFM; SLPM)	106; 3000

TABLE 4.—CAPACITANCE CLEARANCE PROBE SPECIFICATIONS

Calibrated operating maximum temperature	1500 °F
Measurement range (in.)	0 to 0.125
Accuracy (in.)	0.0002
Resolution (in.)	0.00005
Excitation voltage (V)	15
Probe diameter (in)	0.375
Stand-off distance for current tests (in)	0.025
Weight (lb)	0.04
Manufacturer	Capacitec
Model no.	HPC 150

clearance probes were used to measure the radial displacement of the seal carriers (fig. 7) at three different circumferential locations. Table 4 provides a list of the probe specifications. Two capacitance clearance probes were mounted diametrally opposite one another and the third was clocked at 90° relative to the first two.

5. Data Acquisition System

A National Instruments (NI) LabVIEW-based program running on a PC host computer was used to implement data acquisition and stepper motor control. Temperature, pressure, and flow are measured at a rate of two samples per second, and position data (motor encoders and clearance probes) are sampled at 20 samples per second. The data is digitized with a 12 bit analog/digital (A/D) card. The stepper motors are controlled with two 8 axes motion control cards located in a remote chassis. Communication delays between the PC and the chassis limits the control loop time to approximately 50 ms.

6. Control Implementation

The active clearance control system was implemented in NI LabVIEW with an NI motion control blockset that allows the nine stepper motors to be controlled simultaneously via the motion control cards. The advantage of using motion control is that stepper motor "positional moves" commanded by LabVIEW are generated by the motion control cards and hence operate independently of the software (limited to 50 ms updates). When LabVIEW commands a "positional move," a desired position and velocity is fed to the motion control board and the move begins.

The actuators were controlled in either open-loop or closed-loop modes. In open-loop mode, a single position move was commanded to all nine actuators. Motion stops after the commanded number of motor steps have been executed.

Closed loop control was used for evaluating the ability of the ACC system to maintain a tight clearance set-point during simulated engine transients. An on-off set point tracking controller was implemented in LabVIEW to track clearance transients with the stepper motor actuators. An error signal was computed every 50 ms by subtracting the actual clearance (as measured by the proximity probes) from the desired clearance set-point. A position move equal to the magnitude and direction of the error signal was commanded to the stepper motors. If the move completed before 50 ms elapses, then the motor would stop until the next cycle began. If the move did not complete, the motor would remain in motion, but, with updated commands. In order to minimize tracking delays due to error propagation, the motor velocity was set to a value of 0.010 in./sec.

B. Procedures

1. Seal Component Leakage Rates

A goal of the current work is to identify how much each seal component contributes to the overall leakage. This will guide future seal development efforts to reduce component leakages and overall ACC system leakage to their practical

minimums. Low ACC parasitic leakage is required in order to minimize P3 cooling air loss and to net the engine efficiency gains from the tighter tip clearance control.

To quantify the individual leakage levels of each sealing component utilized in the ACC test rig, five different static flow test setups were used. These flow tests were conducted at room temperature using pressure differentials ranging from 0 to 120 psig in 20 psig increments. Each test setup was strategically designed to allow the leakage of each seal component to be isolated from the total leakage of the composite test system as a whole. For the low flow component tests (all except the flexure seals), air was supplied to the system through a 3/8 in. port on the upper chamber cover. Chamber pressure was monitored through a second 3/8 in. cover plate port, and flow rate and an additional pressure measurement were collected from the system air supply line. Each seal utilized in the ACC rig is listed below with a description of the configuration used to quantify its contribution to total system leakage.

C-Seal Leakage Evaluation: To evaluate the performance of the C-seals, system leakage was limited to the outer C-seal on the lower chamber cover. This was achieved by plugging the actuator rod and air inlet ports, placing elastomeric O-rings in the upper cover plate instead of the upper C-seals, and installing a solid aluminum shroud in place of the seal carriers. This shroud was machined to have the same dimensions as the ring of seal carriers normally present in the test chamber, and utilized O-ring seals on both top and bottom to limit chamber pressurization to the outer half of the test chamber. Because the lower C-seals were difficult to remove, they were left in place for all subsequent leakage tests. The leakage rates for those tests were corrected to compensate for the additional leakage path.

Air Inlet Piston Ring Seals: The effectiveness of the air inlet piston ring seals was evaluated using a test setup nearly identical to that used for the C-seal tests; however the plugs were removed from the air inlet ports and replaced with blanked air supply pipes and corresponding piston ring seals. All three air inlet piston ring station leakages were measured simultaneously.

Actuator Rod Piston Ring Seals: To determine the leakage of the actuator rod piston rings, the actuator rods and piston rings were installed in their respective locations and the actuator rod feet were installed. Aluminum spacer blocks were positioned between the outer chamber wall and the back side of each foot to hold the rods in place during pressurization. All three air inlet ports were plugged and the solid shroud and cover plate with O-rings were positioned into their respective locations. Air was supplied through the 3/8 in. port as described earlier.

Face Seals: During face seal testing, both the air inlet and actuator rod ports were plugged, and O-rings were used in the upper cover plate. During these tests, however, the O-rings were removed from the solid shroud and the upper- and lower-face seals sealed against the sides of the solid shroud. The E-seals used to preload the face seals were also installed.

Flexure Seals: The flexure seal leakage was considerably greater than the previous leakage rates. To avoid choking through the 3/8 in. inlet port, air was supplied using one of the 3 air inlet ports. The other two remained capped with their respective O-ring sealed plugs. Due to the higher leakage flow rates, a higher capacity (106 SCFM, 0.143 lbm/s) flow meter (Teledyne Hastings) was used. All other seals were installed for these tests (C-seals, face seals, actuator rod piston rings). The leakage of the flexure seals was extracted from the total leakage data by subtracting the known leakage contributions of the other seals in the system from the composite flow rate. The measured flow is an aggregate for all nine flexure seals.

2. *Effect of Carrier Position on Leakage*

Static Leakage: To gauge the ability of the ACC rig seals to block flow at multiple radial positions, static flow tests were conducted at pressures including 10 and 30 psig. The upper test pressure was limited to 30 psig due to the load capabilities of the stepper motors used for actuation. Open loop actuator control was used. The test chamber was pressurized with the seal carriers in their nominal or "home" position. The nominal position was defined as the diameter established by the alignment fixture shown engaging the seal carrier pins in figure 8. Once pressurized, the seal carriers were actuated radially outward to a position 0.040 in. from the "home" position. Next, the carriers were moved radially inward at a rate of 0.005 in./sec., pausing at three locations (0.035 in. radially outward from the "home," "home," and 0.035 in. radially inward from "home") to collect static leakage values. (For reference purposes, positive sign convention represents movement inward radially from the "home" position). Inward motion was stopped when the carriers reached a location 0.040 in. radially inward from the "home" position. At this point, motion was reversed and leakage values were collected at the same three locations during the outward stroke. This method was applied to determine whether static seal leakage was dependent on the direction of seal carrier travel prior to stopping.

Dynamic Leakage: Dynamic leakage values were gathered using the same open-loop displacement control scheme employed for the static leakage tests described previously. However, instead of stopping to record static leakage values, system leakage was continuously logged (2 Hz) while the seal carriers were actuated through the displacement range. Seal carrier motion was limited to 0.001 in./second, as dictated by the "settling time" of the flow meter used to monitor leakage rates.

3. *Open Loop Positional Accuracy Test*

The ability of the ACC rig to move as directed was evaluated through a series of open loop positional accuracy tests conducted at ambient temperature and pressures of 5,

10, 20, 30, and 35 psig. To start each test, the seal carriers were sent to their nominal position (“home”) and the test chamber was pressurized to the desired test pressure. Once pressurized, positional reference values were collected by measuring the clearance between the actuator rod hard stop couplings and the actuator mounts using gage pins. These reference values were recorded for each of the nine actuator axes. From “home”, the seal carriers were actuated radially inward 0.035 in., back to home, radially outward 0.035 in., and then back again to home (one complete cycle). At each location, positional reference values were recorded using gage pin measurements. The positional reference values were then used to determine whether the actuator rods moved the directed distance. Positional reference measurement accuracy was limited by a 0.001 in. gage pin resolution.

4. *Displacement Repeatability Study*

The ability of the ACC rig to track a series of displacements and then return to the “home” position was evaluated by imposing a commanded sine wave displacement (0.035 in. amplitude) on the system while it was pressurized to 20 psig. Initial reference locations were recorded using gauge pin measurements once the test chamber was pressurized. The seal carriers were actuated radially inward and outward for 20 cycles with the seal carrier speed limited to a maximum of 0.010 in./sec. Post cycling reference measurements were recorded for comparison with the original seal carrier locations.

5. *Control System and Simulated Engine Clearance Versus Time Study*

Figure 10 summarizes the overall control logic strategy used in the ACC test rig system. The control system is composed of an inner loop where the position of each of the nine stepper motors is monitored via encoders. The outer-loop or executive level controls the overall motion of the seal carriers receiving input from three capacitance clearance probes (see table 4 for probe details). The control system constantly checks to see which probe is at the minimum clearance and uses that probe for control for a conservative approach. To investigate the control system’s behavior during transient events such as take-off, desired carrier position (e.g., set point) signals are fed to the control system at the outer-loop level.

During a take-off transient, the rotor expands due to centrifugal loads and blades expand quickly due to combined thermal and centrifugal loads. The case does not expand nearly as fast, and consequently, the ACC system must move the seal carrier segments radially outward against pressure loads to maintain blade-tip clearance. Clearance control must be demonstrated with small tracking errors sufficiently small to avoid blade rubs (0.005-in. or less). A 200-second take-off transient profile representative of a large commercial engine that exhibits a clearance change of 45 mils in 10 seconds was used to demonstrate closed-loop control. Clearance control tests were performed using chamber pressures of 10, 20, and 30 psig.

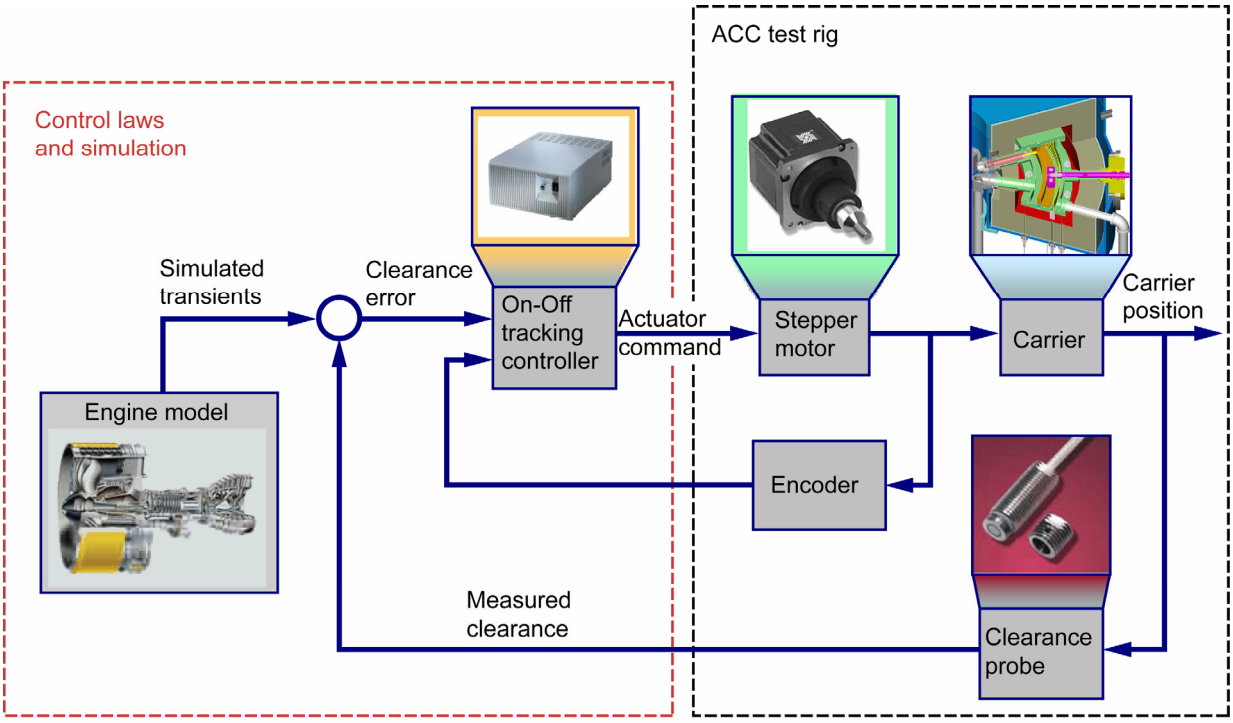

Figure 10.—Closed-loop active clearance control implementation.

III. Results and Discussion

A. Baseline Seal Component Leakage Results

Leakage rates for each of the ACC test rig seals were measured using the procedures described above at ambient temperature. Figure 11 shows air leakage rates and for the most part the leakage rates vary linearly with pressure drop. The flexure seals contribute the majority of the leakage at 85 percent of the total. The face seals contribute the next highest percentage at 7 percent of total flow. The piston rings for the nine actuator rods contribute 6 percent. The rig supporting seals (e.g., air inlet piston rings and the four C-ring seals) contribute approximately 2 percent of the total. Table 3 provides flow measurement accuracies for both the low and high flow ranges examined.

B. Comparison of Effective Seal Flow Area to Industry Reference Level

As stated earlier, low ACC parasitic losses are required to harvest the engine efficiency gains from the tighter tip clearance control. In the current section, we make an initial comparison of the measured losses in terms of effective leakage flow area per inch of circumference to an engine industry reference level.

Using the total measured leakage rates of all seal locations, we back-calculated an effective leakage flow area for the entire active clearance control system, to compare to an engine industry reference level. The method used to back-calculate the effective leakage flow area was taken from an isentropic flow condition with compressibility at the choked-flow condition.[9] The leakage flow was considered choked since the pressure ratio of 8.3 (i.e., $P_{supply}/P_{exhaust}$ = 122.7 psia/14.7 psia) was above the critical pressure ratio for air. The equation used was:

$$\frac{Flow\ Area}{Circumference} = \frac{\dot{m} \times \sqrt{R \times T}}{0.6847 \times \sqrt{g_c} \times P_{supply} \times Circumference}$$

where:

$Flow\ Area$	=	flow area (in^2) where flow is choked
$Circumference$	=	π×Diameter (in.)
$\dot{m}$	=	measured flow rate (lb_m/sec)
R	=	gas constant for air ($53.3\ lb_f\text{-ft} / lb_m\text{-°R}$)
T	=	temperature (°R)
g_c	=	gravitational constant ($32.2\ lb_m\text{-ft}/lb_f\text{-sec}^2$)
P_{supply}	=	supply pressure (psia)

Industry Reference Effective Flow Area: If one were to idealize the ACC system as an elastic structure (e.g., rubber band) that could move radially inward/outward seals would only be required between the sides of the seal carriers and the static structure. Engine designers have acknowledged that flows in these areas less than ~0.1 percent core-flow (W25) would be an acceptable loss considering the potential for the significant gains possible through the tighter HPT tip clearances. Converting this level into an effective flow area per unit circumference results in approximately 0.00048 in^2/in. of circumference. Since there are two seal locations the total effective flow area per unit of circumference would be twice the above or 0.00096 in^2/in. Figure 12 compares the effective flow area per unit circumference found for the rig to this industry reference level. Though this current data is only for ambient conditions, the effective flow area for the ACC rig falls within the industry reference level.

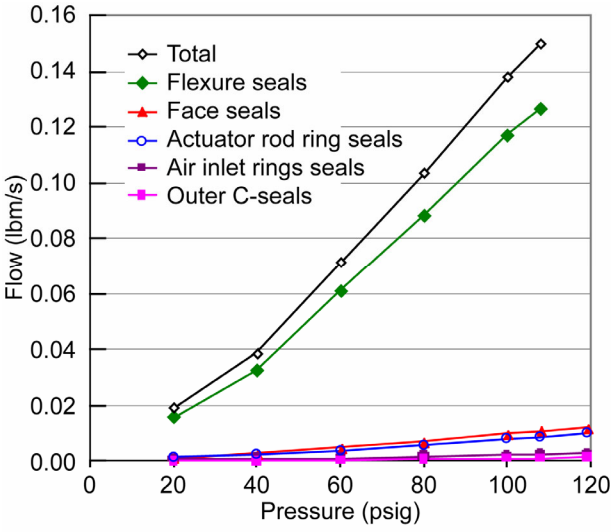

Figure 11.—Seal component leakage rates versus pressure at ambient temperature.

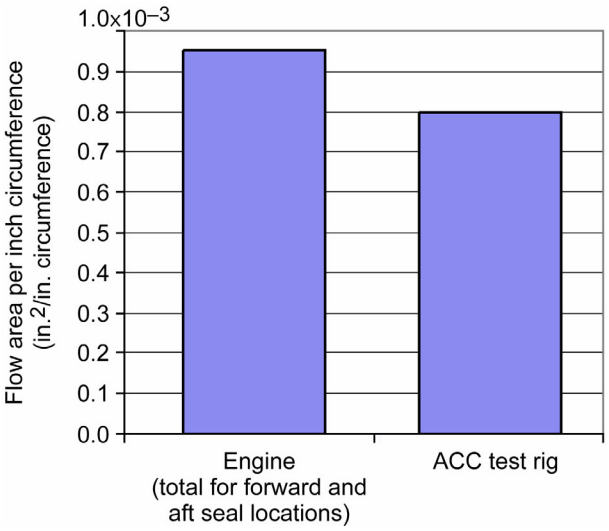

Figure 12.—Comparison of ACC test rig effective flow area per inch circumference (back-calculated from leakage flow data) to engine reference flow area per inch circumference for forward and aft seal locations.

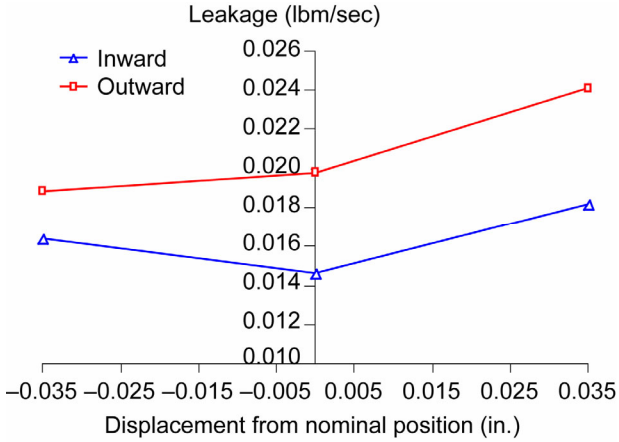

Figure 13.—Flow versus displacement at three carrier radial positions: nominal and displaced ±0.035-in. from nominal. Positive is radially inward. Figure also shows effect of shroud movement-direction (prior to stopping) on leakage rate. Conditions: pressure 30 psig, static condition.

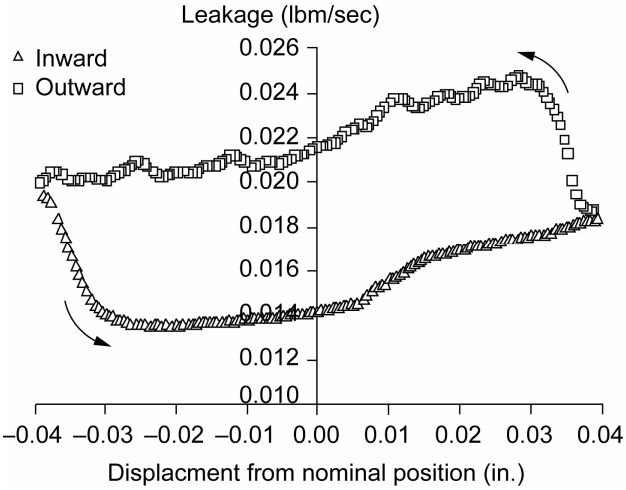

Figure 14.—Flow versus displacement for dynamic test. Positive is radially inward. Figure also shows effect of shroud movement-direction on leakage rate. Conditions: pressure 30 psig, seal shroud moving at 0.001-in./sec.

C. Effect of Seal Carrier Position on ACC Leakage: Static and Dynamic Tests

Figure 13 shows the result of the static leakage versus seal carrier position tests at a chamber pressure of 30 psig. The ACC flow rates show a hysteresis effect and flows are greatest when the seal carriers are closer together and are moving radially outward. The largest difference in the flow is 0.006 lbm/s and occurs at the inward position. This represents about a ±15 percent variation in flow relative to the average flow. The static flow rate at 10 psig is similar to the 30 psig results—just at a lower flow level, as one would expect.

Figure 14 shows the result of the dynamic leakage versus seal carrier position tests at a chamber pressure of 30 psig.

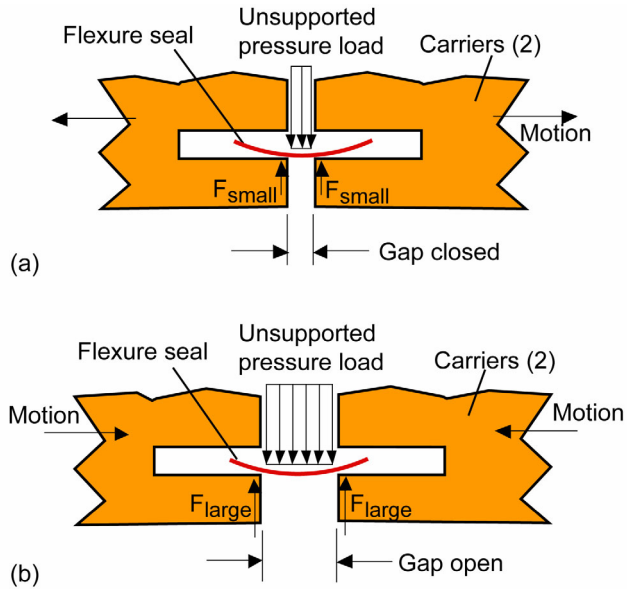

Figure 15.—Diagram of flexure seals in seal carriers in two states. (a) Seal carriers positioned radially-in but moving apart; (b) Seal carriers positioned radially-out but moving toward one another. Note when gap is open the normal loads on the flexure seals are greater. The flexure seal is shown in a deformed condition (enlarged for clarity).

The dynamic leakage again shows a hysteresis effect and is also greatest when the seal carriers are closer together and moving outward radially. Similar to above there is about a ±15 percent variation in flow relative to the average flow. The correlation between static and dynamic leakages indicate no strong dependence on actuation rate, at least at the 0.001 in./sec tested herein. However comparing the dynamic flows from figure 14 (~0.024 lbm/s) to the total static leakage flow in figure 11 (0.03 lbm/s), we note that the dynamic flows are slightly less. A likely explanation is that motion and pressure are seating the seals lowering the leakage flows. The dynamic flow behavior at 10 psig was similar to the 30 psig results—albeit at lower leakages, as would be expected.

Figures 13 and 14 indicate that the ACC flow rates are greater when the seal carriers are closer together than when they are further apart. Figure 15 depicts the a flexure seal supported by two adjacent seal carriers in two states: (a) Seal carriers positioned radially-in but moving apart; (b) Seal carriers positioned radially-out but moving toward one another. A possible explanation for the noted difference in flow appears to be related to the unsupported pressure loads in the two states and the direction of motion. Note when the seal carriers are fully apart, the unsupported area and hence the resultant force is greatest. Under these conditions (e.g., radially outward), the higher flexure seal contact loads would tend to reduce the leakage flows. The direction of motion also seems to play a role in the leakage

flow. One possible explanation is that as the seal carriers are moving toward one another friction loads tend to further increase the contact loads on the slightly deformed flexure (see deformed condition in diagram) in the interface between the flexure seal and the carriers. Another possible explanation is possible leakage-directional dependence of the face seals. Further investigations are required to examine these theories.

D. Open Loop Positional Accuracy Test

Figure 16 shows the results for the open-loop positional accuracy test at a pressure of 20 psig. Results for this pressure are shown as being representative of other pressures tested. In the 20 psig tests the nine stepper motors were issued a command to move the equivalent number of motor steps to move the actuator rods ±0.035 in. from the nominal or "home" position. In this test, the stepper motor encoders were not providing feedback to the controller. Figure 16(a) shows the actuator position as measured with the pin gages. Figure 16(b) shows the error. The maximum error observed for these tests was about 0.003-in. These results indicate evidence of either "slipped counts" or "positional hysteresis" which is typical for open-loop stepper motor operation near their load limit. In the actual application feedback control would be required.

The positional accuracy tests performed herein were done with pressure loading to simulate the "loaded" condition in the application. Without pressure loading open-loop positional accuracy was worse due to small clearances between load train components (or backlash). Without pressure loading backlash up to 0.013 in. was measured.

E. Repeatability Study

The ACC rig was cycled in open-loop position feedback mode to evaluate the system repeatability and ability to return to its nominal or "home" position. In this test, the system was pressurized to 20 psig and cycled 20 times. Carrier positions were measured using three capacitance probes: two diametrally opposite one-another and a third at 90°. Actuator positions were checked using precision pin gages as described in the Test Procedures Section.

Table 5 provides the results of these tests. After 20 cycles all nine actuators returned to their original or "home" position to within ±0.001-in. showing excellent repeatability. For reference purposes, pin gages used were calibrated in 0.001-in. increments so the measured deviation was within the limits of the measuring technique. The convention used herein is positive deviation is radially inward from home and negative deviation is radially outward from the home position. Note that the there is some variation in pre-/post-test position relative to the actuator mount measurements for the nine axes due to slight differences in actuator rod lengths and shims used in the mounting of the stepper motors. This in no way affected the position repeatability results.

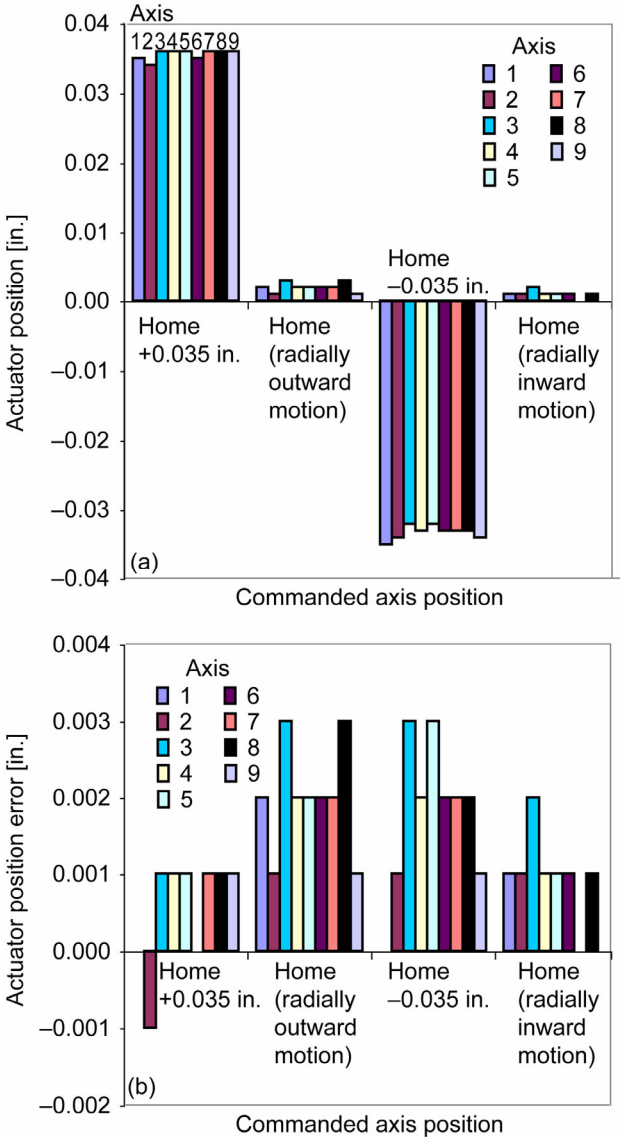

Figure 16.—ACC open-loop position control evaluation for three positions: nominal and ±0.035-in. for a complete cycle. (a) Actuator position measured using manual pin gages, (b) Positional error: commanded versus actual. Conditions: pressure 20 psig, ambient temperature. Sign convention: positive error indicates inward radial relative to the commanded position.

F. Simulated Engine Clearance Versus Time Study

Figure 17 shows the result of the simulated engine clearance versus time study where the set-point position defines ideal carrier position movement versus time for a simulated take-off condition. These tests were performed at a pressure of 20 psig. Figure 17(a) shows the set-point and the measured carrier position at three clock positions: probe 1(0°), probe 2 (90°), probe 3 (180°). Throughout these tests the controller examined all three probes and controlled

TABLE 5.—REPEATABILITY TEST RESULTS: CONDITIONS: 20 CYCLES STARTING AT NOMINAL POSITION, MOVING ±0.035-in. FROM NOMINAL POSITION AND RETURNING HOME. 20 psig PRESSURE, AMBIENT TEMPERATURE. ERROR IS DIFFERENCE IN POSITION BEFORE AND AFTER TEST

Individual Actuator Axis Position			
Axis number	Pre-test position relative to actuator mount (in.)	Post-test position relative to actuator mount (in.)	Error (in.)
1	0.356	0.356	0.000
2	0.416	0.415	0.001
3	0.423	0.424	–0.001
4	0.345	0.345	0.000
5	0.393	0.393	0.000
6	0.404	0.404	0.000
7	0.390	0.389	0.001
8	0.428	0.428	0.000
9	0.403	0.404	–0.001
Individual Capacitance Probe Clearance			
Probe number	Pre-test clearance (in.)	Post-test clearance (in.)	Error (in.)
1	0.051	0.051	0.000
2	0.054	0.054	0.000
3	0.053	0.053	0.000

Notes:
- Positive deviation is radially inward from home and negative deviation is radially outward from the home position.
- Probe 1 and 3 are diametrically opposed. Probe 2 is clocked 90° between probes 1 and 3.

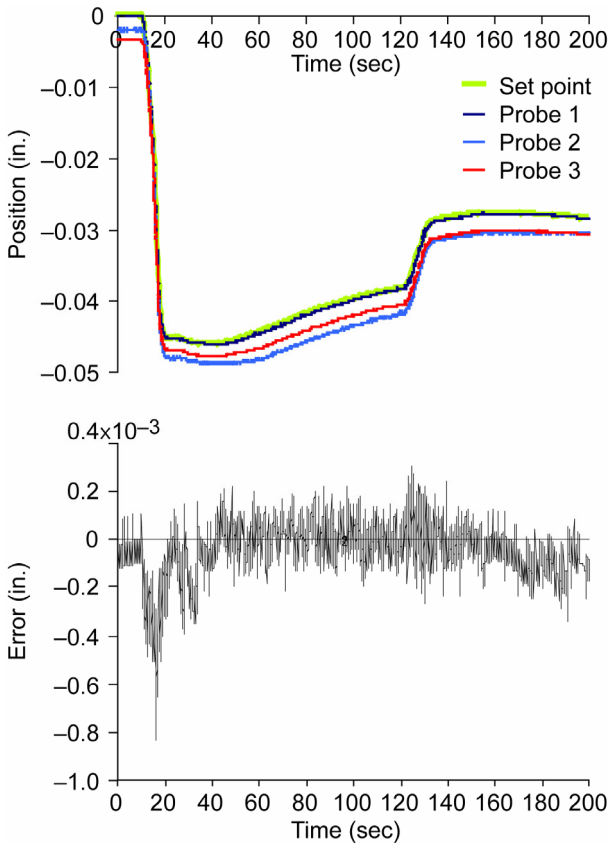

Figure 17.—ACC test rig simulation of engine clearance transient during take-off conditions. (a) Commanded (e.g., set point) and measured carrier position (using capacitance probes). Negative position indicates movement radially outward from start position or simulated "flight idle" condition; (b) Positional error versus time. Conditions: pressure 20 psig, ambient temperature, control based on minimum clearance of 3 capacitance probes.

to the minimum clearance which in this case was at probe 1. Though it may difficult to see, the motion of the carrier adjacent probe 1 tracked the set-point very well. The carriers adjacent the other two probes were slightly further away from the probes from assembly set-up and those carriers remained further outward radially throughout the test.

Figure 17(b) shows the error defined as "set-point minus actual position" on a highly refined vertical scale. (Note that for this chart, negative error indicates the actuator did not move outward radially as far as the set-point). For the entire simulated take-off transient, the error between the set-point (green line) and probe data (black line) was less than 0.001-in. This was a very encouraging result as it showed that this kinematic system could track simulated engine clearance changes at the correct rate and range under load with an acceptable error. Note: Tests were also performed at chamber pressures of 10 and 30 psig. The results were generally the same except that the error tracked with pressure. This is the expected result as the higher (e.g., 30 psig) pressure load and corresponding frictional effects were just above what the stepper motor could reliably actuate without slowing down. Future hydraulic actuators are designed to overcome this shortcoming.

IV. Summary and Conclusions

An active clearance control system concept and associated test rig has been fabricated and installed. The system is being used to evaluate different kinematic, actuator, controller, and clearance-sensor approaches to achieve a fast-acting, mechanical active clearance control system to allow tighter turbine tip clearances in future turbine engines. The current study investigated the abilities of the ACC system concept to control leakage to acceptable levels and to position seal carriers at the appropriate

actuation rates and accuracies. The current study investigated the system performance at appropriate pressure differentials but at ambient temperature. Future studies will examine performance under engine simulated pressures and temperatures.

Based on the tests performed herein, the following observations are made:

- The kinematic system permits movement of the seal carriers over a range of 0.080-in. This range easily accommodates the anticipated range required for future turbine engines.
- The system leakage was tested at pressures up to 120 psig—comparable to pressure differentials anticipated in future engines. Leakage unit flow area was comparable to an engine industry reference level.
- The system repeatability was examined at the limit of the stepper motor loads (20 psig pressure loads) showing that after 20 cycles (±0.035 in. inward/outward radial movement) that the positional error was within the 0.001-in. resolution of the gage pin measurement technique.
- Tests showed that the closed-loop position control followed the set-point to less than 0.001-in. for a simulated engine take-off clearance change with capacitance clearance probes in the loop. This was an encouraging result as it showed the kinematic system could track simulated clearance changes at the correct rate and range under load with an acceptable error.

References

[1]Halila, E.E., Lenahan, D.T., Thomas, T.T., "Energy Efficient Engine, High Pressure Turbine Test Hardware Detailed Design Report," NASA CR-167955, 1982.

[2]Lattime, Scott L., Steinetz, Bruce M., "Turbine Engine Clearance Control Systems: Current Practices and Future Directions," Journal of Propulsion and Power, vol. 20, no. 2, NASA/TM—2002-211794, also AIAA–2002–3790, presented at the AIAA/ASME/SAE/ASEE conference, July, 2002, Indianapolis, IN.

[3]Kawecki, E.J., "Thermal Response Turbine Shroud Study," Air Force Aero Propulsion Laboratory Technical Report AFAPL–TR–79–2087, 1979.

[4]Melcher, K.J., and Kypuros, J.A., "Toward a Fast-Response Active Turbine Tip Clearance Control," Proceedings of the XVI International Symposium on Air Breathing Engines, Cleveland, OH, August 31–September 5, 2003.

[5]DeCastro, J.A., Melcher, K.M., "A Study on the Requirements for Fast Active Turbine Tip Clearance Control Systems," Proceedings of the 40th Joint Propulsion Conference and Exhibit, AIAA–2004–4176, 2004.

[6]Lattime, S.L., Steinetz, Bruce M., Robbie, M., "Test Rig for Evaluating Active Turbine Blade Tip Clearance Control Concepts," NASA/TM—2003-212533, also AIAA–2003–4700, presented at the AIAA/ASME/SAE/ASEE conference, July, 2003, Huntsville, AL. Journal of Propulsion and Power, vol. 21 (3) May-June 2005.

[7]General Electric Aircraft Engines, "HPT Clearance Control (Intelligent Engine Systems)—Phase I—Final Report" NASA Contract NAS3–01135, April 2004.

[8]Wiseman, M.W., Guo, T., "An Investigation of Life Extending Control Techniques for Gas Turbine Engines," Proceedings of the American Control Conference, IEEE Service Center, Piscataway, NJ, IEEE Catalog No. 01CH37148, vol. 5, pp. 3706–3707, 2001.

[9]Shapiro, Ascher H., The Dynamics and Thermodynamics of Compressible Flow, The Ronald Press Co., New York, 1953.

REPORT DOCUMENTATION PAGE

Form Approved
OMB No. 0704-0188

1. AGENCY USE ONLY (*Leave blank*)	2. REPORT DATE	3. REPORT TYPE AND DATES COVERED
	November 2005	Technical Memorandum

4. TITLE AND SUBTITLE

Evaluation of an Active Clearance Control System Concept

5. FUNDING NUMBERS

WBS–22–714–92–56

6. AUTHOR(S)

Bruce M. Steinetz, Scott B. Lattime, Shawn Taylor, Jonathan A. DeCastro, Jay Oswald, and Kevin J. Melcher

7. PERFORMING ORGANIZATION NAME(S) AND ADDRESS(ES)

National Aeronautics and Space Administration
John H. Glenn Research Center at Lewis Field
Cleveland, Ohio 44135–3191

8. PERFORMING ORGANIZATION REPORT NUMBER

E–15226

9. SPONSORING/MONITORING AGENCY NAME(S) AND ADDRESS(ES)

National Aeronautics and Space Administration
Washington, DC 20546–0001

10. SPONSORING/MONITORING AGENCY REPORT NUMBER

NASA TM—2005-213856
AIAA–2005–3989

11. SUPPLEMENTARY NOTES

Prepared for the 41st Joint Propulsion Conference and Exhibit cosponsored by the AIAA, ASME, SAE, and ASEE, Tucson, Arizona, July 10–13, 2005. Bruce M. Steinetz and Kevin J. Melcher, NASA Glenn Research Center; Scott B. Lattime, The Timken Company, 1835 Dueber Ave. SW, Canton, Ohio 44706; Shawn Taylor, University of Toledo, 2801 W. Bancroft Street, Toledo, Ohio 43606; Jonathan A. DeCastro, QSS Group, Inc., 21000 Brookpark Road, Cleveland, Ohio 44135; and Jay Oswald, J&J Technical Solutions, 14880 Timber Lane, Cleveland, Ohio 44130. Responsible person, Bruce M. Steinetz, organization code RSM, 216–433–3302.

12a. DISTRIBUTION/AVAILABILITY STATEMENT

Unclassified - Unlimited
Subject Category: 37

Available electronically at http://gltrs.grc.nasa.gov

This publication is available from the NASA Center for AeroSpace Information, 301–621–0390.

12b. DISTRIBUTION CODE

13. ABSTRACT ***(Maximum 200 words)***

Reducing blade tip clearances through active tip clearance control in the high pressure turbine can lead to significant reductions in emissions and specific fuel consumption as well as dramatic improvements in operating efficiency and increased service life. Current engines employ scheduled cooling of the outer case flanges to reduce high pressure turbine tip clearances during cruise conditions. These systems have relatively slow response and do not use clearance measurement, thereby forcing cold build clearances to set the minimum clearances at extreme operating conditions (e.g., takeoff, reburst) and not allowing cruise clearances to be minimized due to the possibility of throttle transients (e.g., step change in altitude). In an effort to improve upon current thermal methods, a first generation mechanically-actuated active clearance control (ACC) system has been designed and fabricated. The system utilizes independent actuators, a segmented shroud structure, and clearance measurement feedback to provide fast and precise active clearance control throughout engine operation. Ambient temperature performance tests of this first generation ACC system assessed individual seal component leakage rates and both static and dynamic overall system leakage rates. The ability of the nine electric stepper motors to control the position of the seal carriers in both open- and closed-loop control modes for single and multiple cycles was investigated. The ability of the system to follow simulated engine clearance transients in closed-loop mode showed the system was able to track clearances to within a tight tolerance (≤ 0.001 in. error).

14. SUBJECT TERMS	15. NUMBER OF PAGES
Seal; Active clearance control; Design; Leakage; Flow; Actuator; Clearance sensor; Turbine; High pressure turbine	20
	16. PRICE CODE

17. SECURITY CLASSIFICATION OF REPORT	18. SECURITY CLASSIFICATION OF THIS PAGE	19. SECURITY CLASSIFICATION OF ABSTRACT	20. LIMITATION OF ABSTRACT
Unclassified	Unclassified	Unclassified	